

Nature of oxygen dopant-induced states in high-temperature $\text{Bi}_2\text{Sr}_2\text{CaCu}_2\text{O}_{8+x}$ superconductors: A photoemission investigation

P. Richard,^{1,*} Z.-H. Pan,¹ M. Neupane,¹ A. V. Fedorov,² T. Valla,³ P. D. Johnson,³ G. D. Gu,³ W. Ku,³
Z. Wang,¹ and H. Ding¹

¹*Department of Physics, Boston College, Chestnut Hill, Massachusetts 02467, USA*

²*Advanced Light Source, Lawrence Berkeley National Laboratory, Berkeley, California 94720, USA*

³*Condensed Matter Physics and Materials Science Department, Brookhaven National Laboratory, Upton, New York 11973, USA*

(Received 20 April 2006; published 26 September 2006)

We investigate the nature of oxygen dopant-induced electronic states in the high-temperature $\text{Bi}_2\text{Sr}_2\text{CaCu}_2\text{O}_{8+x}$ superconductor by measuring photoemission spectra of underdoped, optimally doped, and overdoped samples using a wide photon energy range (15–100 eV). We find a small and broad nondispersive peak at -0.8 eV associated with oxygen dopants. Surprisingly, the detailed analysis of the resonance profile suggests a mixing with Cu states. Particularly, the A_{1g} symmetry revealed by polarization-dependent experiments and the comparison with the single-layered $\text{Bi}_2\text{Sr}_2\text{CuO}_{6+x}$ indicates that the oxygen dopant-induced states are mixed to the superconducting CuO_2 planes through the oxygen dopant—apical oxygen $O_a 2p_z$ — $\text{Cu} 3d_{3z^2-r^2}$ channel.

DOI: [10.1103/PhysRevB.74.094512](https://doi.org/10.1103/PhysRevB.74.094512)

PACS number(s): 74.72.Hs, 74.25.Jb, 79.60.-i

The unexpected finding of nanoscale electronic disorder evidenced by scanning tunneling spectroscopy (STS) is one of the most remarkable features of cuprates, and it may hold the key in the understanding of high-temperature superconductivity.¹ For this reason, the origin of the electronic inhomogeneities in these materials is the subject of intense debates. By correlating STS spectra to the local electronic disorder as a function of doping, a recent study of the high-temperature superconductor $\text{Bi}_2\text{Sr}_2\text{CaCu}_2\text{O}_{8+x}$ (Bi2212) has established the in-plane position of the oxygen dopants (O_δ) in this compound.² Particularly, the differential conductance at the O_δ site is characterized by a broad peak around -0.96 eV.² Even though STS measurements point towards an oxygen dopant-induced origin of the electronic disorder in cuprates,^{1,2} the nature of the dopant-induced states and how they couple to the superconducting CuO_2 planes are still unknown. Solving this important issue is an essential step and sheds light on the mechanism of high-temperature superconductivity.

Owing to their atomic selectivity, resonant photoemission experiments can provide unique and valuable insights concerning the wave function of the states of interest. We present in this paper a photoemission study of Bi2212 which reveals a small, broad, and nondispersing peak corresponding to a localized state around -0.8 eV. We show that the spectral weight of the corresponding peak increases with doping, indicating its relation to the presence of O_δ . In order to characterize the nature of this dopant-induced state, we utilized the “element-resolved” capability of photoemission experiments by measuring spectra for a wide photon energy range. The peak exhibits photon energy resonances around 50 eV and 75 eV. Surprisingly, the latter corresponds to the $\text{Cu} 3p \rightarrow 3d$ edge, suggesting a mixing of the localized state with Cu. Furthermore, the absence of resonance associated with the $\text{O} 2s \rightarrow 2p$ transition implies that the state can only involve fully ionized oxygens. Using different light polarizations, we show that the peak is likely to have A_{1g} symmetry. This suggests that the oxygen dopant-induced states ob-

served are mixed with the $\text{Cu} 3d_{3z^2-r^2}$ orbitals of the superconducting planes through the $O_a 2p_z$ - $\text{Cu} 3d_{3z^2-r^2}$ hybridization (O_a =apical oxygen), rather than with the Zhang-Rice singlet.³ This interpretation is consistent with the lack of a similar feature in $\text{Bi}_2\text{Sr}_2\text{CuO}_{6+x}$ (Bi2201), in which the $O_a 2p_z$ - $\text{Cu} 3d_{3z^2-r^2}$ is found ~ 1 eV higher in binding energy according to our theoretical calculation. This mixing suggests that the O_δ - $O_a 2p_z$ - $\text{Cu} 3d_{3z^2-r^2}$ channel plays an important role in the CuO_2 local electronic disorder.

High-quality single crystals of Bi2212 with various doping have been grown by the traveling solvent floating zone method and subsequently annealed. For the sake of clarity, we use in the text the notation XT to identify the doping level of the samples. In this shortened notation, X refers to underdoped (UD), optimally doped (OP) or overdoped (OD) samples, while T corresponds to the superconducting temperature. For example, OD71 means an overdoped sample with $T_c=71$ K. ARPES spectra at 20 K were measured with photon energy from 28 to 100 eV, using a Scienta SES-100 and the synchrotron beamline 12.001 of the Advanced Light Source, CA. For these measurements, the rotating capability of both the sample holder and the analyzer allowed us to record spectra with polarization parallel or perpendicular to $\Gamma(0,0)$ - $Y(\pi,\pi)$ and $M(0,\pi)$ - Y on the same samples. We also checked that the same features around -1.0 eV are observed in the Γ - $X(-\pi,\pi)$ configuration, which presents no superstructure. Measurements were also obtained at 10 K for the 15–23 eV photon energy range using a Scienta SES-2002 and the synchrotron beamline U13UB of the National Synchrotron Light Source, NY. The energy resolution is ~ 10 – 40 meV for the photon energy range used in this study. Samples have been cleaved and measured *in situ* in a vacuum better than 8×10^{-11} Torr on a flat (001) surface and degradation of the spectra with time has not been observed.

The complementarity of the ARPES and STS techniques suggests that ARPES spectra should exhibit fingerprints of the -0.96 eV STS peak associated with O_δ . Besides normalization and matrix element effects, the space-integrated STS

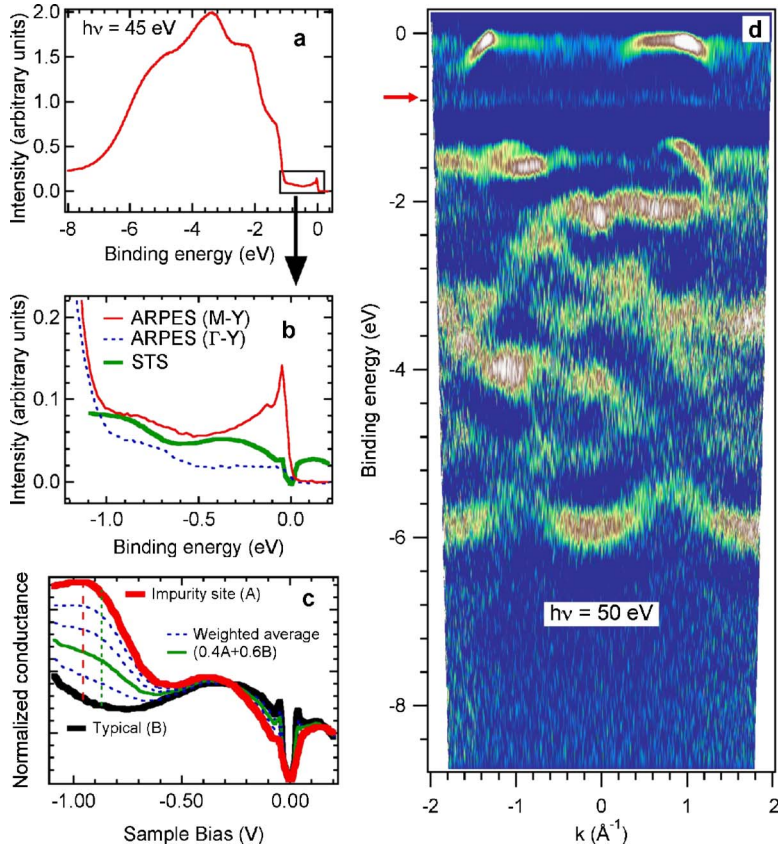


FIG. 1. (Color online) (a) A k_F -centered EDC of an OD71 sample along M-Y. (b) A zoom of the M-Y (thin plain line) and Γ -Y (dotted line) EDCs at k_F compared to the weighted average of the STS typical (60%) and O_δ site (40%) spectra (thick line) from Ref. 2. (c) Weighted averages (20% steps) of the typical and O_δ site STS spectra from Ref. 2. The left vertical dashed line and right vertical dotted line correspond to the -0.96 eV STS peak and to the slope change from the weighted curve (third curve from the bottom), respectively. (d) The second derivative intensity plot of an OP90 sample along Γ -M.

spectrum should be similar to the momentum-integrated ARPES one, since both of these integrated spectra are proportional to the density of states. Also, a nondispersive peak observed in a spectra obtained by integrating along symmetry lines should also appear in the density of states. As illustrated in Fig. 1(a), a small and broad peak is revealed in the energy distribution curve (EDC) of an OD71 sample obtained at a photon energy of 45 eV within a 0.3 \AA^{-1} momentum window centered at the k_F point (we refer to this as k_F -centered throughout the paper) of the anti-nodal direction (M-Y). A zoom of this EDC around -1.2 and 0.2 eV is given in Fig. 1(b). In order to illustrate the effect of space averaging on the -0.96 eV STS peak and to reproduce the ARPES results, we show in Fig. 1(c) weighted averages (20% steps) of the two STS curves digitized from Fig. 1(a) in Ref. 2. The third curve from the bottom (60% typical spectrum +40% impurity site spectrum⁴) is reproduced in Fig. 1(b). A good qualitative agreement is found between this curve and the OD71 k_F -centered EDCs measured along the nodal and antinodal directions. As the weight of the STS impurity state spectrum decreases and the spectrum evolves to the typical STS spectrum, the peak is smoothly suppressed and manifests its presence by a slope change rather than a well defined maximum. Even though the exact position of the slope change depends on the normalization procedure of the STS spectra, it is always observed at lower binding energies than the -0.96 eV peak.⁵ This is illustrated in Fig. 1(c) by the dotted line associated with the weighted STS curve slope change. Interestingly, the -0.8 eV ARPES peak does not show any dispersion, as illustrated by the second derivative intensity plot shown in Fig. 1(d), in contrast to most of the

other bands detected in the -7.0 to 0.3 eV energy range. This is consistent with the local impurity state origin of the feature.

The correspondence between the -0.8 eV ARPES feature and the -0.96 eV STS peak, which has been associated with the O_δ , is reinforced by its doping dependence. A typical doping evolution is given in Fig. 2(a), where the EDCs of UD70, OP90 and OD71 samples are compared. The intensity of the -0.8 eV peak increases with the doping x . In order to obtain quantitative information, we extracted the weight of the -0.8 eV peak using the following procedure, illustrated in the inset of Fig. 2(a). After normalization of each EDC to the total spectral weight of the -8.0 to $+0.1$ eV binding energy range, we extracted a cubic polynomial background to the logarithm of the EDCs. Due to the strong tail of the valence band and the weakness of the -0.8 eV peak, the use of the logarithm of the EDCs rather than the EDCs improved the fits. Then, we converted back the background obtained into the natural scale (dotted curve) and calculated the area under the peak by subtracting the two curves in the -1.05 to -0.55 eV range. The errors have been estimated by evaluating how the background varies with different fit parameters and by considering the signal/noise ratio. Figure 2(b) shows, as a function of doping, the results obtained by averaging the weight extracted from the EDCs measured in the 28–100 eV photon energy range (circles). The doping x , and thus the amount of O_δ , has been deduced from the empirical relation⁶ between T_c and x given by $T_c^{\text{max}}/T_c = 1 - 82.6(x - 0.16)^2$ with $T_c^{\text{max}} = 95$ K (plain curve). The weight extracted is consistent with the relation proportional to x (dashed line) expected for the interpretation of the -0.8 eV local state in terms of O_δ .

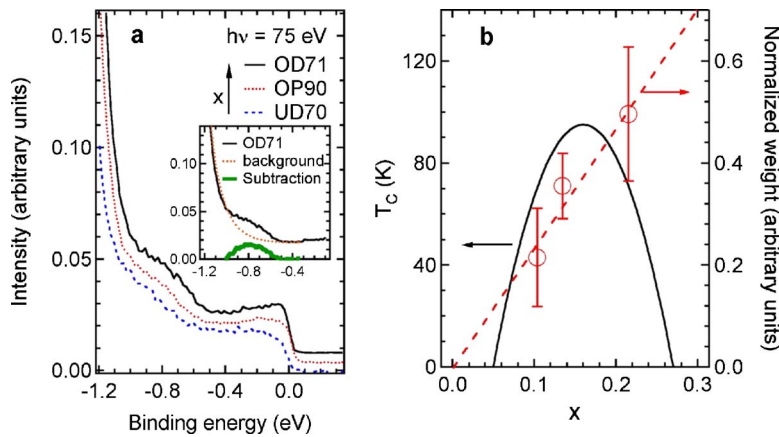


FIG. 2. (Color online) (a) The k_F -centered EDCs of the UD70 (bottom), OP90 (middle) and OD71 (top) samples EDCs obtained along Γ -Y. Inset: background (dotted curve) associated with the OD71 EDC and the subtraction of the two curves (thick line). (b) Doping dependence of the -0.8 eV peak spectral weight (circles), empirical relation (plain) between T_c and the doping x given in Ref. 6 ($T_c^{\max}=95$ K), and proportional relation between the spectral weight and x (dashed line).

We now ask the question: How does the O_δ couple to the in-plane electronic properties? We investigated the electronic character of the -0.8 eV peak by performing ARPES measurements in a wide photon energy range, which are summarized in Fig. 3. The k_F -centered EDCs along the nodal direction are shown in panels (a) and (b). While the impurity state peak does not show any dispersion, its amplitude exhibits some photon energy dependence. Interestingly, the peak is particularly intense and well defined for photon energies around 45–50 and 75–80 eV. Even though the situation is less clear for the low photon energy range (15–23 eV), a change of slope in the EDCs is clearly seen in the -1.0 to -0.5 eV range, as illustrated in Fig. 3(b). Using the procedure described above, we extracted the weight associated with the -0.8 eV peak for a wide range of photon energy.

Figures 3(c) and 3(d) show, for the 15–23 eV and 28–100 eV photon energy ranges, respectively, the results obtained for UD, OP, and OD samples. The average error bars are also indicated in these figures. The weight extracted is consistent with the precedent observations. Hence, sharp resonances are observed around 50 eV and 75 eV. As for the low energy range, no resonance can be defined, within the error bars.

The -0.8 eV peak resonance around 75 eV suggests that this peak is, surprisingly, related to copper ions. It is well known that the $Cu3p$ core levels locate around -75 eV,^{7–10} and we observed them at -76.7 and -75.1 eV in our OD71 sample. Thus, one can expect that such photon energy would enhance the direct transition $Cu3p^63d^9+h\nu\rightarrow Cu3p^63d^8+e^-$ due to an interference with a super Coster-Kronig Auger de-

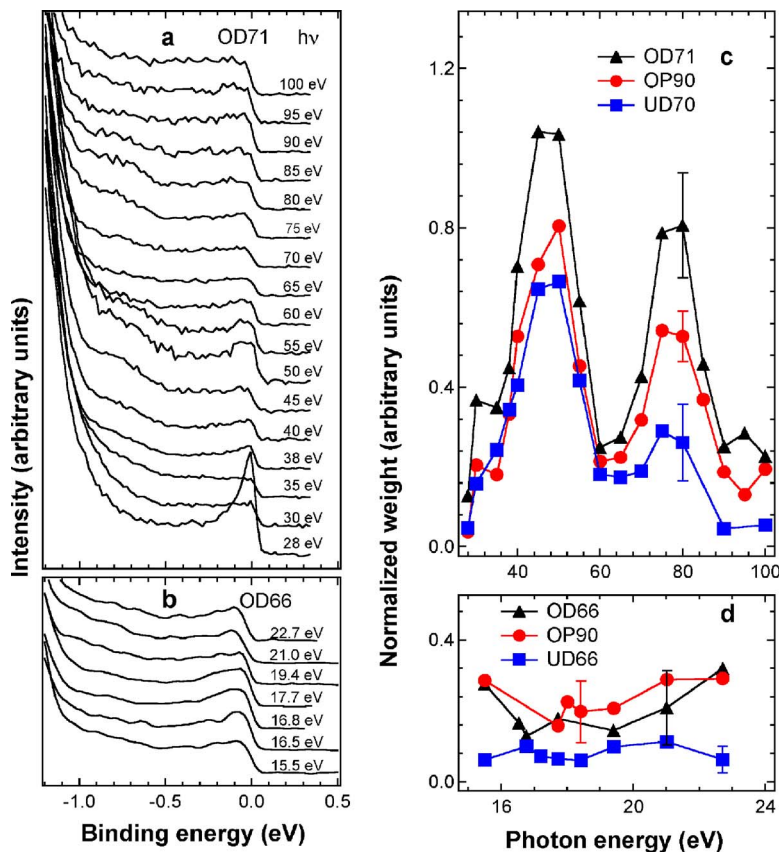


FIG. 3. (Color online) The nodal k_F -centered EDCs are given in (a) for an OD71 sample using the high photon energy range (28–100 eV) and in (b) for an OD66 sample using the low photon energy range (15–23 eV). The corresponding weight of the -0.8 eV peak is given in panels (c) and (d) for the high and low photon energy ranges, respectively.

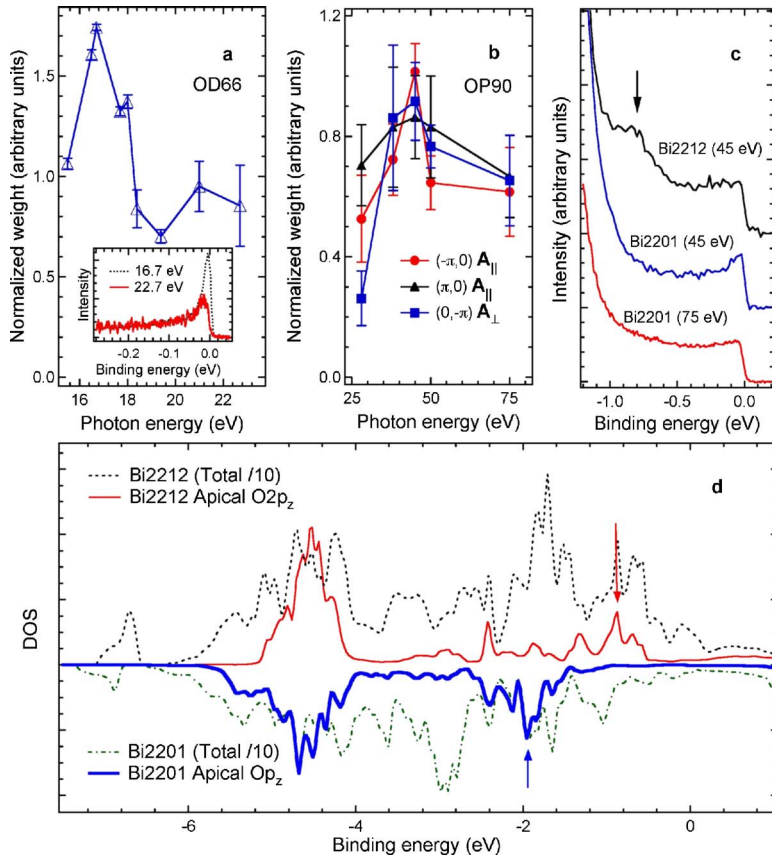


FIG. 4. (Color online) (a) Photon energy dependence of the nodal quasi-particle peak weight. Inset: Comparison between the nodal k_F EDCs obtained at 16.7 eV (dotted line) and 22.7 eV (plain line). (b) Polarization dependence of the -0.8 eV spectral weight. (c) Comparison between the Bi2201 (OD7) and Bi2212 (OP91) M -centered EDCs. (d) Calculated total and $O_a 2p_z$ density of states for Bi2201 and Bi2212.

cay process described by $Cu3p^6 3d^9 + h\nu \rightarrow Cu3p^5 3d^{10} \rightarrow Cu3p^6 3d^8 + e^-$.¹¹ It is well established that $Cu3p^6 3d^8$ represents a satellite state (~ -12.5 eV) of the valence band, as observed in $La_{2-x}Sr_xCuO_4$ and $YBa_2Cu_3O_{6+x}$.¹⁰ In our OD71 sample, this satellite is observed at -12.3 eV and we checked that it is also strongly enhanced at a photon energy of 75 eV as compared to 70 eV. Contrary to the 75 eV resonance, the resonance around 50 eV is more difficult to interpret in terms of a copper resonance. However, previous ARPES studies of Bi2212 revealed a resonance of the anti-bonding component of the bilayer hybridization around 50 eV.^{12,13} Thus, the 50 eV resonance observed for the -0.8 eV peak and the near E_F anti-bonding band resonance may be related. Remarkably, we observed no indication of any resonance associated directly with oxygen, as one would expect. For example, such a resonance, reinforced by quantum interference with the $O2s \rightarrow O2p$ transition (around 17–18 eV¹⁴), enhances the near- E_F band along the nodal direction, as shown in Fig. 4(a). However, it has no sizable effect on the -0.8 eV peak intensity [see Fig. 3(d)]. This indicates that the local state observed involves only oxygens with filled $2s$ and $2p$ shells (O^{-2}).

Even though the localized state observed at -0.8 eV is induced by the O_δ , its precise origin remains unclear. The most natural explanation of our results is to interpret the -0.8 eV peak as an O_δ level. A recent DFT study has established that the O_δ site is most likely located between the SrO and BiO layers,¹⁵ with a small ab displacement as compared to the STS results.² It has been concluded from LDA calculations performed on the relaxed structure obtained by DFT

that the feature observed by STS, and thus by ARPES, comes from the unhybridized dopant $O2p_z$ states.¹⁵ However, this hypothesis cannot explain the photon energy resonances observed by ARPES. In an alternative scenario, the -0.8 eV peak can be interpreted as O_δ states strongly mixed with their environment. The O_δ is likely to be mixed with Cu through the $O_a 2p_z$ and $Cu3d_{3z^2-r^2} A_{1g}$ orbitals. The absence of strong polarization dependence illustrated in Fig. 4(b) is consistent with this scenario and disfavors the possibility of a mixing of the -0.8 eV local state with the Zhang-Rice singlet ($Cu3d_{x^2-y^2}$ and $O2p_{x,y}$ bands).³ In order to investigate further this second scenario, the total density of states (DOS) and the DOS of the $O_a 2p_z$ band have been calculated for both Bi2201 and Bi2212 using LDA+U. As indicated by the results, given in Fig. 4(d), the DOS of the $O_a 2p_z$ band in Bi2212 exhibits a significant feature around -1 eV (indicated by arrows), which is moved by about 1 eV towards the higher binding energies in Bi2201. As a consequence, the absence of the -0.8 eV peak in the experimental overdoped Bi2201 EDC (OD7) illustrated in Fig. 4(c) suggests that this peak comes from spectral weight pulled out from the valence band, following the mixing of the O_δ with the $O_a 2p_z$ band, which is itself hybridized to the $Cu3d_{3z^2-r^2}$ band. Moreover, the complementarity between ARPES and STS allows us to predict that the -0.96 eV peak observed by STS will not be observed in Bi2201.

Among the possible consequences of the second scenario proposed above, a local modification of the Cu-Cu second nearest neighbor hopping term t' is expected since the $Cu3d_{3z^2-r^2}$ and $O_a 2p_z$ orbitals related to this parameter are

themselves strongly perturbed in the vicinity of the impurity site. This leads to correlations between the O_δ distribution and the CuO_2 electronic properties, as evidenced by the gap magnitude inhomogeneities reported by STS.² However, it is not clear that the observed weight of the -0.8 eV resonance can account for all oxygen dopants. Actually, a careful counting of the impurity sites observed by STS indicates that only a fraction of the dopants (~ 0.5) are detected,² suggesting the possibility of additional O_δ nonequivalent sites for which the ARPES and STS techniques are not sensitive.

In summary, we have investigated the nature of oxygen dopant-induced states found at -0.8 eV by measuring ARPES spectra in a wide photon energy range. Surprisingly, the resonance profile of the corresponding nondispersive peak indicates an unexpected mixing with Cu states. More-

over, the A_{1g} symmetry of the peak and the comparison with the single-layered $\text{Bi}_2\text{Sr}_2\text{CuO}_{6+x}$ suggests that the oxygen dopant-induced states are mixed with Cu through the $O_\delta\text{-O}_a2p_z\text{-Cu}3d_{3z^2-r^2}$ channel, providing a better understanding of the origin of the local electronic disorder in cuprates.

We thank J. C. Davis, P. J. Hirschfeld, P. A. Lee, and F. C. Zhang for valuable discussions and suggestions. This work is supported by NSF Grant No. DMR-0353108 and DOE Grant No. DE-FG02-99ER45747. This work is based upon research conducted at the National Synchrotron Light Source supported by DOE Contract No. DE-AC02-98CH10886 and at the Advanced Light Source supported by DOE Contract No. DE-AC03-76SF00098.

*Electronic address: richarpi@bc.edu

¹S. H. Pan, J. P. O'Neal, R. L. Badzey, C. Chamon, H. Ding, J. R. Engelbrecht, Z. Wang, H. Eisaki, S. Uchida, A. K. Gupta, K.-W. Ngk, E. W. Hudson, K. M. Lang, and J. C. Davis, *Nature (London)* **413**, 282 (2001).

²K. McElroy, J. Lee, J. A. Slezak, D.-H. Lee, H. Eisaki, S. Uchida, and J. C. Davis, *Science* **309**, 1048 (2005).

³F. C. Zhang and T. M. Rice, *Phys. Rev. B* **37**, 3759 (1988).

⁴Assuming an amount of 0.11 O_δ per CuO_2 plane resulting from the doping of an overdoped sample ($x=0.22$) and the ~ 4 Å radius of the impurity site (Ref. 2), 37% of the sample surface is covered by impurity sites.

⁵Different normalization procedures can change the ratio R of the impurity site and typical spectrum intensities around -1 eV. A decrease of R moves the slope change to lower binding energies.

⁶M. R. Presland, J. L. Tallon, R. G. Buckley, R. S. Liu, and N. E. Flower, *Physica C* **176**, 95 (1991).

⁷M. Iwan, F. J. Himpsel, and D. E. Eastman, *Phys. Rev. Lett.* **43**, 1829 (1979).

⁸M. R. Thuler, R. L. Benbow, and Z. Hurych, *Phys. Rev. B* **26**, 669 (1982).

⁹G. Wendin, *J. Phys. Colloq.* **48**, 1157 (1987).

¹⁰Z.-X. Shen, J. W. Allen, J. J. Yeh, J.-S. Kang, W. Ellis, W. Spicer, I. Landau, M. B. Maple, Y. D. Dalichaouch, M. S. Torikachvili, J. Z. Sun, and T. H. Geballe, *Phys. Rev. B* **36**, 8414 (1987).

¹¹L. C. Davis, *Phys. Rev. B* **25**, 2912 (1982).

¹²A. A. Kordyuk, S. V. Borisenko, T. K. Kim, K. A. Nenkov, M. Knupfer, J. Fink, M. S. Golden, H. Berger, and R. Follath, *Phys. Rev. Lett.* **89**, 077003 (2002).

¹³S. V. Borisenko, A. A. Kordyuk, T. K. Kim, A. Koitzsch, M. Knupfer, M. S. Golden, J. Fink, M. Eschrig, H. Berger, and R. Follath, *Phys. Rev. Lett.* **90**, 207001 (2003).

¹⁴H. M. Meyer and J. H. Weaver, *Physical Properties of High Temperature Superconductors II*, edited by D. M. Ginsberg (World Scientific, Singapore, 1990).

¹⁵Y. He, T. S. Nunner, P. J. Hirschfeld, and H.-P. Cheng, *Phys. Rev. Lett.* **96**, 197002 (2006).